

Siberian Branch of Russian Academy of Sciences

BUDKER INSTITUTE OF NUCLEAR PHYSICS

R.R. Akhmetshin, E.V. Anashkin, M. Arpagaus,  
V.M. Aulchenko, V.Sh. Banzarov, L.M. Barkov, N.S. Bashtovoy,  
A.E. Bondar, D.V. Bondarev, A.V. Bragin, D.V. Chernyak,  
A.G. Chertovskikh, A.S. Dvoretzky, S.I. Eidelman,  
G.V. Fedotovitch, N.I. Gabyshev, A.A. Grebeniuk,  
D.N. Grigoriev, V.W. Hughes, P.M. Ivanov, S.V. Karpov,  
V.F. Kazanin, B.I. Khazin, I.A. Koop, M.S. Korostelev,  
P.P. Krokovny, L.M. Kurdadze, A.S. Kuzmin, I.B. Logashenko,  
P.A. Lukin, A.P. Lysenko, K.Yu. Mikhailov, A.I. Milstein,  
I.N. Nesterenko, V.S. Okhapkin, A.V. Otboev,  
E.A. Perevedentsev, A.A. Polunin, A.S. Popov, T.A. Purlatz,  
N.I. Root, A.A. Ruban, N.M. Ryskulov, A.G. Shamov,  
Yu.M. Shatunov, A.I. Shekhtman, B.A. Shwartz, A.L. Sibidanov,  
V.A. Sidorov, A.N. Skrinsky, V.P. Smakhtin, I.G. Snopkov,  
E.P. Solodov, P.Yu. Stepanov, A.I. Sukhanov, J.A. Thompson,  
V.M. Titov, A.A. Valishev, Yu.V. Yudin, S.G. Zverev

**$a_1(1260)\pi$  dominance in the process  
 $e^+e^- \rightarrow 4\pi$  at energies 1.05–1.38 GeV**

Budker INP 98-83

Novosibirsk

1998

# $a_1(1260)\pi$ dominance in the process $e^+e^- \rightarrow 4\pi$ at energies 1.05–1.38 GeV

R.R. Akhmetshin, E.V. Anashkin, M. Arpagaus, V.M. Aulchenko,  
V.Sh. Banzarov, L.M. Barkov, N.S. Bashtovoy, A.E. Bondar,  
D.V. Bondarev, A.V. Bragin, D.V. Chernyak, A.G. Chertovskikh,  
A.S. Dvoretzky, S.I. Eidelman, G.V. Fedotovitch, N.I. Gabyshev,  
A.A. Grebeniuk, D.N. Grigoriev, P.M. Ivanov, S.V. Karpov, V.F. Kazanin,  
B.I. Khazin, I.A. Koop, M.S. Korostelev, P.P. Krokovny, L.M. Kurdadze,  
A.S. Kuzmin, I.B. Logashenko, P.A. Lukin, A.P. Lysenko, K.Yu. Mikhailov,  
A.I. Milstein, I.N. Nesterenko, V.S. Okhapkin, A.V. Otboev,  
E.A. Perevedentsev, A.A. Polunin, A.S. Popov, T.A. Purlatz, N.I. Root,  
A.A. Ruban, N.M. Ryskulov, A.G. Shamov, Yu.M. Shatunov,  
A.I. Shekhtman, B.A. Shwartz, A.L. Sibidanov, V.A. Sidorov,  
A.N. Skrinsky, V.P. Smakhtin, I.G. Snopkov, E.P. Solodov, P.Yu. Stepanov,  
A.I. Sukhanov, V.M. Titov, A.A. Valishev, Yu.V. Yudin, S.G. Zverev  
Budker Institute of Nuclear Physics, Novosibirsk, 630090, Russia

J.A.Thompson  
University of Pittsburgh, Pittsburgh, PA 15260, USA

V.W.Hughes  
Yale University, New Haven, CT 06511, USA

## Abstract

First results of the study of the process  $e^+e^- \rightarrow 4\pi$  by the CMD-2 collaboration at VEPP-2M are presented for the energy range 1.05–1.38 GeV. Using an integrated luminosity of  $5.8 pb^{-1}$ , energy dependence of the processes  $e^+e^- \rightarrow \pi^+\pi^-2\pi^0$  and  $e^+e^- \rightarrow 2\pi^+2\pi^-$  has been measured. Analysis of the differential distributions demonstrates the dominance of the  $a_1\pi$  and  $\omega\pi$  intermediate states. Upper limits for the contributions of other alternative mechanisms are also placed.

# 1 Introduction.

Investigation of  $e^+e^-$  annihilation into hadrons at low energies provides unique information about interaction of light quarks and spectroscopy of their bound states. At present the energy range below  $J/\psi$  can not be satisfactorily described by QCD. Future progress in our understanding of the phenomena in this energy range is impossible without accumulation of experimental data vitally important to check the predictions of existing theoretical models. In addition, the total cross section of  $e^+e^-$  annihilation into hadrons at low energies as well as the cross sections of exclusive channels are necessary for precise calculations of various effects. These include strong interaction contributions to vacuum polarization for  $(g-2)_\mu$  and  $\alpha(M_Z^2)$  [1], tests of standard model by the hypothesis of conserved vector current (CVC) relating  $e^+e^- \rightarrow$  hadrons to hadronic  $\tau$ -lepton decays [2, 3], determination of the QCD parameters based on QCD sum rules [4] etc.

The energy behavior of the total cross section as well as that of the cross sections for exclusive channels is complicated and characteristic of various broad overlapping resonances (e.g.  $\rho, \omega, \phi$  recurrences) with numerous common decay channels having energy thresholds just in this energy range. Presence of the broad resonances in the intermediate state necessitates consideration of the quasistationary states and makes effects of their interference important.

Until recently the investigation of  $e^+e^-$  annihilation into hadrons was restricted by measurements of the cross sections only. Appearance of the new detectors with a large solid angle operating at high luminosity colliders and providing very large data samples opens qualitatively new possibilities for the investigation of the multihadronic production in  $e^+e^-$  annihilation.

Production of four pions is one of the dominant processes of  $e^+e^-$  annihilation into hadrons in the energy range from 1.05 to 2.5 GeV. For the first time it was observed in Frascati [5] and Novosibirsk [6]. First experiments with limited data samples allowed one to qualitatively study the new phenomenon of multiple production of hadrons and estimate the magnitude of the corresponding cross sections. Subsequent measurements by different groups in Frascati, Orsay and Novosibirsk (see the references in [1]) provided more detailed information on the energy dependence of the cross sections of the processes  $e^+e^- \rightarrow 2\pi^+2\pi^-$  and  $e^+e^- \rightarrow \pi^+\pi^-2\pi^0$  in comparison with the previous measurements.

One of the main difficulties in the experimental studies of four pion production was caused by the existence of different intermediate states via which

the final state could be produced, such as

$$e^+e^- \rightarrow \omega\pi \quad (1)$$

$$e^+e^- \rightarrow \rho\sigma \quad (2)$$

$$e^+e^- \rightarrow a_1(1260)\pi \quad (3)$$

$$e^+e^- \rightarrow h_1(1170)\pi \quad (4)$$

$$e^+e^- \rightarrow \rho^+\rho^- \quad (5)$$

$$e^+e^- \rightarrow a_2(1320)\pi \quad (6)$$

$$e^+e^- \rightarrow \pi(1300)\pi \quad (7)$$

The relative contributions of the above mentioned processes can't be obtained without the detailed analysis of the process dynamics. First attempts of this type were performed by MEA [7] and DM1 [8] in the energy range above 1.4 GeV and OLYA [9] and CMD [10] below 1.4 GeV and it was shown that the  $2\pi^+2\pi^-$  final state is dominated by the  $\rho^0\pi^+\pi^-$  mechanism. ND [11] measured the cross section of  $\omega\pi$  production from 1.0 to 1.4 GeV with a magnitude which was confirmed by the subsequent  $\tau$  decay studies at ARGUS [12] as well as by more recent results from CLEO [13] and ALEPH [14].

Later the DM2 group tried to perform partial wave analysis (PWA) of the mode with four charged pions [15] in the energy range 1.35 to 2.40 GeV. Their analysis was based on the momentum distributions only while the angular dependence as well as interference between different waves were not taken into account. Although they obtained some evidence for the presence of  $a_1(1260)\pi$  and  $\rho\sigma$  states, a mechanism for a substantial part of the cross section was not determined. PWA for the mode  $\pi^+\pi^-2\pi^0$  was not performed because of the insufficient number of completely reconstructed events.

The abundance of various possible mechanisms and their complicated interference results in the necessity of simultaneous analysis of two possible final states ( $2\pi^+2\pi^-$  and  $\pi^+\pi^-2\pi^0$ ) which requires a general purpose detector capable of measuring energies and angles of both charged and neutral particles. The first detector of this type operating in the energy range below 1.4 GeV is the CMD-2 detector at VEPP-2M collider in Novosibirsk [16]. In this work, we present results from a model-dependent analysis of both possible channels in  $e^+e^-$  annihilation into four pions based on data collected with the CMD-2 detector. To describe four pion production we used a simple model assuming quasitwoparticle intermediate states and taking into account the important effects of the identity of the final pions as well as the interference of all possible amplitudes.

## 2 Data sample and event selection

The analysis described here is based on  $5.8 \text{ pb}^{-1}$  of  $e^+e^-$  data collected at center-of-mass energies  $2E_{beam}$  from 1.05 up to 1.38 GeV. The data were recorded at the VEPP-2M  $e^+e^-$  collider of the Budker Institute of Nuclear Physics in Novosibirsk, Russia with the CMD-2 detector in 1997. The energy range mentioned above was scanned twice with a step of 20 MeV: first by increasing energy from 1.05 to 1.37 GeV and then by decreasing energy from 1.38 to 1.06 GeV.

The CMD-2 is a general purpose detector consisting of a drift chamber (DC) with about  $250 \mu$  resolution transverse to the beam and proportional Z-chamber used for trigger, both inside a thin ( $0.4 X_0$ ) superconducting solenoid with a field of 1 T. Photons are detected in the barrel CsI calorimeter with 8-10 % energy resolution and the endcap BGO calorimeter with 6 % energy resolution. More details on the detector can be found elsewhere [16].

### 2.1 Event selection

The present analysis is based on completely reconstructed  $\pi^+\pi^-2\pi^0$  events. At the initial stage, events with one primary vertex with two opposite sign tracks and four or more reconstructed photons were selected. Both tracks should come from the interaction region: a distance from the track trajectories to the beam axis should be less than 0.3 cm and the vertex position along the beam axis should be inside  $\pm 10$  cm. To reject background from collinear events, the acollinearity angle between tracks in the  $R - \phi$  plane should be greater than 0.1 radians. Both tracks are required in the DC fiducial volume: a  $\theta$  angle should be inside  $0.54 \div \pi - 0.54$  radians. Clusters of energy deposition that are not matched with charged track projection are paired to form  $\pi^0$  candidates. These showers must have energies greater than 20 MeV, and invariant mass of the photon pair must lie within  $3\sigma$  of the  $\pi^0$  mass where  $\sigma$  varies between  $(5 \div 10)$  MeV. After that a kinematic fit was performed assuming the  $\pi^+\pi^-2\pi^0$  hypothesis for all possible  $\pi^0$  pairs. For further analysis the combination with  $\min(\chi^2)$  was selected under the condition  $\chi^2/ndf < 2.5$ . After such selection 22128 events remained in the energy range under study.

### 2.2 Final event sample

To understand the dynamics of the process we studied the distribution over the recoil mass for one of the  $\pi^0$ 's. Figure 1 shows this distribution at the

beam energy of 690 MeV. Each event gives two entries to the histogram corresponding to two  $\pi^0$ . A signal from the  $\omega\pi^0$  final state is clearly seen. Points with errors are the data while the smooth line is our fit corresponding to the sum of a Breit-Wigner  $\omega$  signal convoluted with detector resolution and a smooth combinatorial background. The detector contribution to the signal width is about 10 MeV. The number of events under the  $\omega$  peak accounts for only  $\sim 60\%$  of the observed events that indicates at the existence of additional intermediate states.

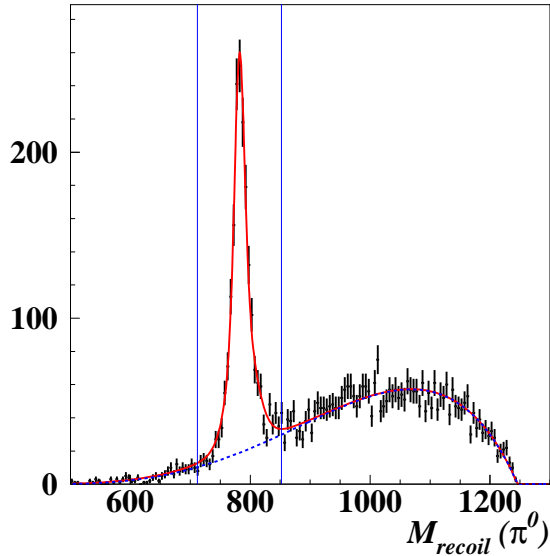


Figure 1: Distribution over the  $\pi^0$  recoil mass for  $\pi^+\pi^-2\pi^0$

For further analysis the data sample was subdivided into two classes:

- I.  $\min(|M_{recoil}(\pi^0) - M_\omega|) < 70 \text{ MeV}$
- II.  $\min(|M_{recoil}(\pi^0) - M_\omega|) > 70 \text{ MeV}$

where  $M_\omega$  is the  $\omega$  mass. The first class contains mostly  $\omega\pi^0$  events while their admixture in the second class is relatively small, about  $(1 \div 5)\%$  depending on the beam energy.

Figs. 2 and 3 show distributions over  $M_{inv}(\pi^\pm\pi^0)$  and  $M_{inv}(\pi^+\pi^-)$  for the events in the second class. In the spectrum of  $M_{inv}(\pi^\pm\pi^0)$  one can see a clear signal of  $\rho^\pm$  while that for  $M_{inv}(\pi^+\pi^-)$  is relatively smooth and no signal from the  $\rho^0$  is observed. The solid lines show our fit including smooth combinatorial background and gaussian  $\rho$  signals. Presence of the  $\rho^\pm$  signal and absence of the  $\rho^0$  signal lead us to the natural assumption that  $\rho$  mesons originate from an isospin 1 resonance. For the case of the resonance with  $I = 0$  one expects production of both neutral and charged  $\rho$ 's.

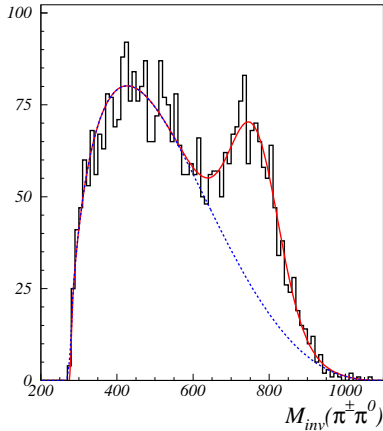


Figure 2: Distribution over  $M_{inv}(\pi^\pm\pi^0)$  for  $\pi^+\pi^-2\pi^0$  events from the class (II)

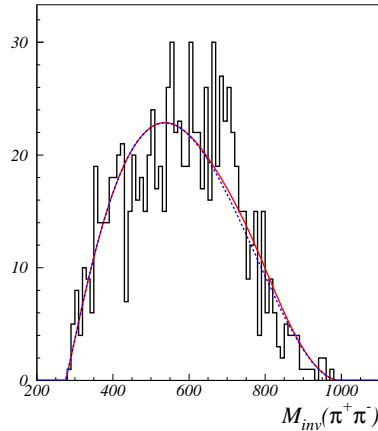


Figure 3: Distribution over  $M_{inv}(\pi^+\pi^-)$  for  $\pi^+\pi^-2\pi^0$  events from the class (II)

Possible candidates from the list of the processes (1)-(7) are  $a_1(1260)$ ,  $a_2(1320)$  and  $\pi(1300)$ . These resonances have different spin and parity resulting in different angular distributions for a recoil pion (Table 1).

Table 1: List of  $I = 1$  resonances with expected angular distributions

		$J^{PC}$	$d\sigma/d\cos(\theta)$	$\chi^2/ndf$
1	$a_1(1260)$	$1^{++}$	$const$	7.1/7
2	$\pi(1300)$	$0^{-+}$	$\sin^2(\theta)$	47.3/7
3	$a_2(1320)$	$2^{++}$	$1 + \cos^2(\theta)$	37.0/7

To measure the angular distribution of the  $\rho^\pm\pi^0$  system (or recoiled  $\pi^\mp$ ) we fit the  $\rho^\pm$  signal in eight ranges of the recoil  $\pi^\mp$  angle with respect to the beam axis. The measured angular distribution is shown in Fig. 4. Three smooth curves show the fits corresponding to mentioned above hypotheses. The fit goodness is presented in the last column of Table 1. One can see good agreement with the hypothesis of the  $a_1(1260)\pi$  intermediate state.

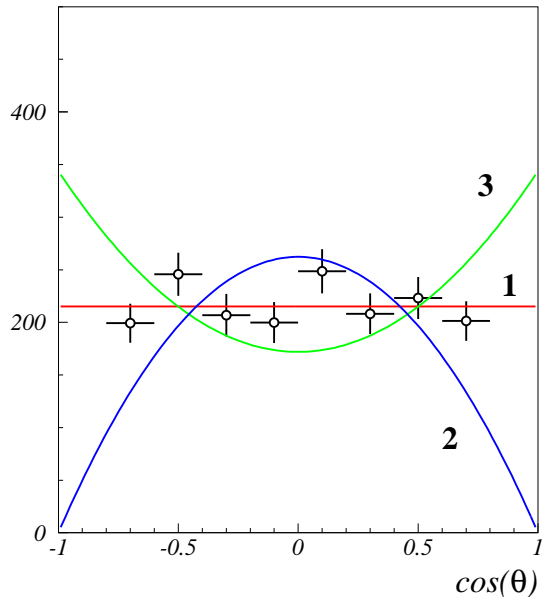


Figure 4: Angular distribution of the recoil  $\pi^\pm$ . Solid curves correspond to the following hypotheses: **1** –  $a_1(1260)\pi$ ; **2** –  $\pi(1300)\pi$ ; **3** –  $a_2(1320)\pi$

Thus one can assume that our data can be explained by  $\omega\pi^0$  and  $a_1(1260)\pi$  intermediate states although small admixture of other states is not excluded.

### 2.3 Fitting method

For detailed comparison we perform the simulation of the processes (1)-(7) taking into account their interference as well as the interference of the diagrams differing by permutations of identical final pions (see Appendix A).

In order to extract a relative fraction of  $a_1(1260)\pi$  and any other intermediate states, the unbinned maximum likelihood fit has been used [17].



Kinematics of each event is completely described by a set of measured four-momenta  $p_\pi \equiv (\varepsilon, \vec{\mathbf{p}})$  of the final pions with the exception of smearing due to detector resolution and radiative effects. This set will be referred to as a vector of state  $\vec{P}_i \equiv (p_{\pi^+}, p_{\pi^-}, p_{\pi^0}, p_{\pi^0})_i$  where a subscript  $i$  stands for the event number.

The theoretical probability density function for  $\vec{P}_i$  depends on process dynamics and can be expressed via the matrix element  $|\mathfrak{M}(\vec{P}_i, \vec{A})|^2$ . Here  $\vec{A}$  stands for a set of unknown model parameters like relative strength and phase of interference between the intermediate states. To obtain the optimal values of  $\vec{A}$  we minimize [18] the logarithmic likelihood function

$$L(\vec{A}) = - \sum_{i=1}^{N_2} \ln w(\vec{P}_i, \vec{A}), \quad (8)$$

where  $w(\vec{P}_i, \vec{A})$  is the probability to observe an event in state  $\vec{P}_i$ , and  $N_2$  is the number of events in the second class. Since the detector resolution for the invariant mass of three pions is about 10 MeV, i.e. comparable to the  $\omega$  width, smearing effects are significant for the events of the first class. Therefore we use the events of the second class only. To fix the fraction of events in the first class we add the following term to the function (8)

$$\frac{(r(\vec{A}) - r_1)^2}{2\sigma_{r_1}^2},$$

where  $r_1 = \frac{N_1}{N_1+N_2}$  is a measured fraction,  $N_1$  is the number of events in the first class, and  $r(\vec{A})$  is the expectation of  $r_1$ .

The normalized probability density function is expressed via the matrix element

$$w(\vec{P}_i, \vec{A}) = \frac{|\mathfrak{M}(\vec{P}_i, \vec{A})|^2}{\sigma_{vis}(\vec{A})} \cdot \frac{1}{\prod_j 2\varepsilon_j},$$

where  $j$  is the particle number, and  $\sigma_{vis}(\vec{A})$  is a model dependent visible cross section:

$$\sigma_{vis}(\vec{A}) = \int |\mathfrak{M}(\vec{P}_i, \vec{A})|^2 \cdot \prod_{j=1}^4 \frac{d^3\vec{\mathbf{P}}_j}{2\varepsilon_j}.$$

The function  $\sigma_{vis}(\vec{A})$  is calculated using Monte Carlo technique. For this purpose we use a set of events sampled according to the relativistic phase

space distribution. In this case,  $\sigma_{vis}(\vec{A})$  is calculated as

$$\sigma_{vis}(\vec{A}) = \frac{1}{N_{MC}} \sum_{i=1}^{N_{MC}} |\mathfrak{M}(\vec{P}_i, \vec{A})|^2,$$

where  $N_{MC}$  is the number of second class events in a generated set.

The main goal of our fits was to find the minimal model compatible with our data. To this end, we write the matrix element as follows:

$$|\mathfrak{M}(\vec{P}_i, \vec{A})|^2 = |\mathbf{J}_{\omega\pi^0}^{+-00} + Z_{a_1} \cdot \mathbf{J}_{a_1\pi}^{+-00} + Z_X \cdot \mathbf{J}_X^{+-00}|^2,$$

where  $X$  stands for an admixture under study —  $\rho\sigma$ ,  $h_1(1170)\pi$ ,  $\rho^+\rho^-$ ,  $a_2(1320)\pi$  or  $\pi(1300)\pi$ . In the above equation, expressions for  $\mathbf{J}_X^{+-00}$  are taken from Appendix A while complex factors  $Z$  are components of the vector  $\vec{A}$ .

## 2.4 Comparison of $\pi^+\pi^-2\pi^0$ data with simulation

Since the matrix element for the channel  $\omega\pi^0$  has a well-known structure, one can use the events from the first class to test the adequacy of the total MC simulation [19]. Figs. 5,6 show the distributions over  $M_{inv}(\pi^\pm\pi^0)$ ,  $M_{recoil}(\pi^\pm)$ ,  $M_{inv}(\pi^+\pi^-)$ ,  $M_{inv}(\pi^0\pi^0)$ ,  $\cos(\psi_{\pi^\pm\pi^0})$ ,  $\cos(\psi_{\pi^+\pi^-})$ ,  $\cos(\psi_{\pi^0\pi^0})$  and  $M_{recoil}(\pi^0)$  for the events of the first class at the beam energy of 690 MeV. Points with errors are the data, while the histograms correspond to the simulation of the processes  $\omega\pi^0$  and  $a_1(1260)\pi$ . Good consistence of the data and MC makes us confident that MC simulation adequately reproduces both the kinematics of produced particles and the detector response to them.

Similar distributions for the events of the second class are shown in Figs. 7,8. One can see that the process  $\pi^+\pi^-2\pi^0$  is satisfactorily described in the minimal model in which there are two intermediate states  $\omega\pi^0$  and  $a_1(1260)\pi$  only. Similar consistence is observed at other energies: we have also examined the energy points  $2E_{beam} = (1.28 \pm 0.01)$  and  $(1.18 \pm 0.03)$  GeV.

To determine the admixture of other possible mechanisms we extend the minimal model above by adding each of the other states one by one and performing the fit. The results of these fits are shown in Table 2. From its third column one can see that the relative fractions  $r_X$  of the additional intermediate state  $X$  with respect to the  $a_1(1260)\pi$  are small. This confirms our assumption of the  $a_1(1260)\pi$  dominance.

Because of the theoretical uncertainty of the  $a_1(1260)\pi$  matrix element, we do not consider the nonnegligible magnitude of the  $\rho^+\rho^-$  and  $\pi(1300)\pi$

Table 2: The results of fit to different models with upper limits

Model	$L_{min}/N_{ev}$	$r_X, \%$	Upper limit, %
$\omega\pi^0 + a_1\pi$	1264/891	—	—
$\omega\pi^0 + a_1\pi + \rho\sigma$	1256/891	$2.1^{+1.2}_{-0.9}$	4.3
$\omega\pi^0 + a_1\pi + h_1\pi$	1263/891	$0.1^{+0.2}_{-0.1}$	0.4
$\omega\pi^0 + a_1\pi + a_2\pi$	1263/891	$0.2^{+0.4}_{-0.2}$	0.8
$\omega\pi^0 + a_1\pi + \pi'\pi$	1250/891	$9.5^{+3.2}_{-2.8}$	15.
$\omega\pi^0 + a_1\pi + \rho^+\rho^-$	1246/891	$4.7^{+2.0}_{-1.6}$	7.7

contributions as significant. Instead, we prefer to set upper limits for the fraction of these intermediate states. The values of the likelihood function (8) for optimal parameters ( $L_{min}$ ) do not contradict to our expectation based on the simulation of  $\omega\pi^0$  and  $a_1(1260)\pi$ .

## 2.5 Comparison of $2\pi^+2\pi^-$ data with simulation

Consider now the  $2\pi^+2\pi^-$  channel. In this case we don't have  $\omega\pi^0$  in the intermediate state and therefore no additional complicacy to check the assumption of the  $a_1(1260)\pi$  dominance arises. To this end four-track events were selected. All tracks should come from the interaction region: a distance from track trajectories to the beam axis should be less than 1 cm and the vertex position along the beam axis should be inside  $\pm 15$  cm. After that a kinematic fit was performed assuming the  $2\pi^+2\pi^-$  hypothesis and events with  $\chi^2/ndf < 2.5$  were selected. Under these conditions 28552 events remain in the energy range under study.

Figure 9 shows distributions over  $M_{inv}(\pi^+\pi^-)$ ,  $M_{inv}(\pi^\pm\pi^\pm)$ ,  $M_{recoil}(\pi^\pm)$  and  $\cos(\psi_{\pi^+\pi^-})$  for  $2\pi^+2\pi^-$  case. One can see that the hypothesis of the  $a_1(1260)\pi$  dominance does not contradict to the data although one should note a slight deviation in the spectrum of the invariant masses of the likesign pions. This deviation can be possibly explained by the contribution of the  $D$ -wave or some final state interaction. It can't be explained by the admixture of other possible processes because their fractions compared to  $a_1(1260)\pi$  are small (see Table 2). The study of more complicated cases taking into account simultaneously a few intermediate states in addition to  $\omega\pi^0$  and  $a_1(1260)\pi$  is now in progress.

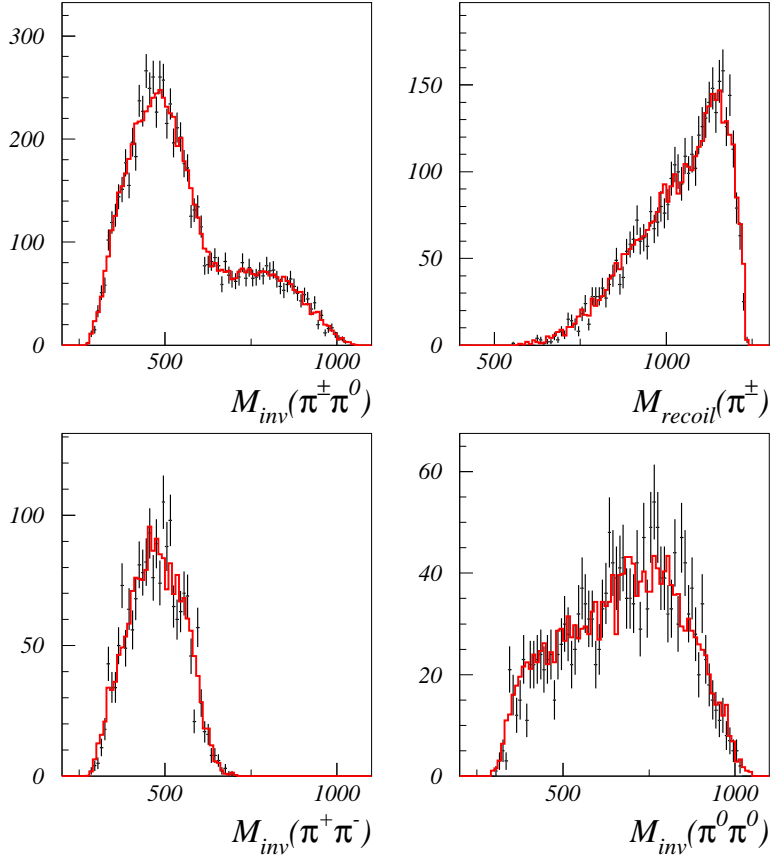


Figure 5: Distributions over  $M_{inv}(\pi^\pm\pi^0)$ ,  $M_{recoil}(\pi^\pm)$ ,  $M_{inv}(\pi^+\pi^-)$ ,  $M_{inv}(\pi^0\pi^0)$  for  $\pi^+\pi^-2\pi^0$  events from the class (I)

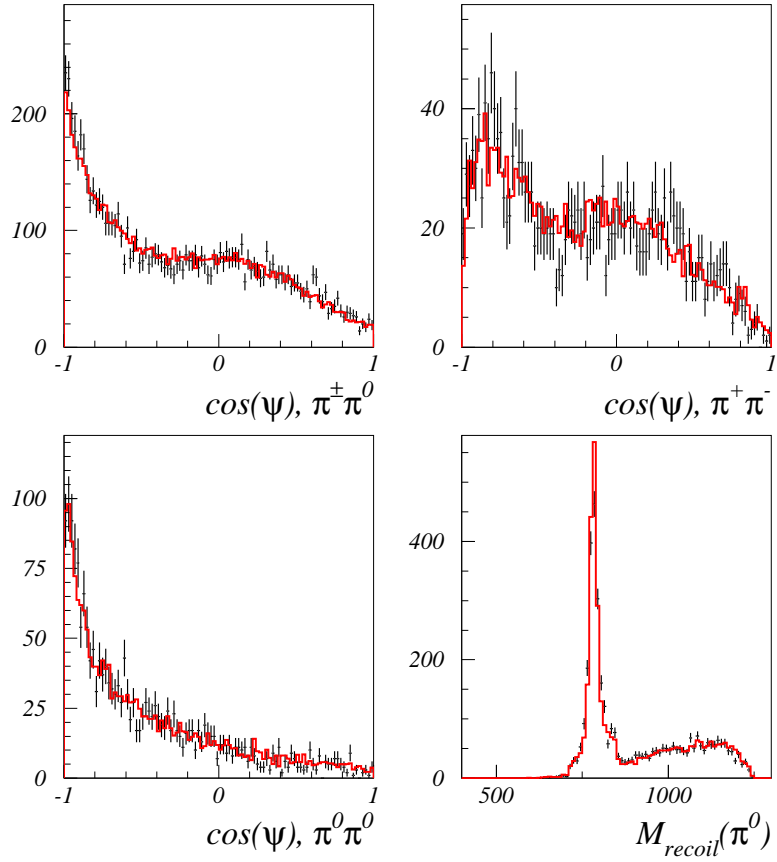


Figure 6: Distributions over  $\cos(\psi_{\pi^\pm\pi^0})$ ,  $\cos(\psi_{\pi^+\pi^-})$ ,  $\cos(\psi_{\pi^0\pi^0})$  and  $M_{recoil}(\pi^0)$  for  $\pi^+\pi^-2\pi^0$  events from the class (I)

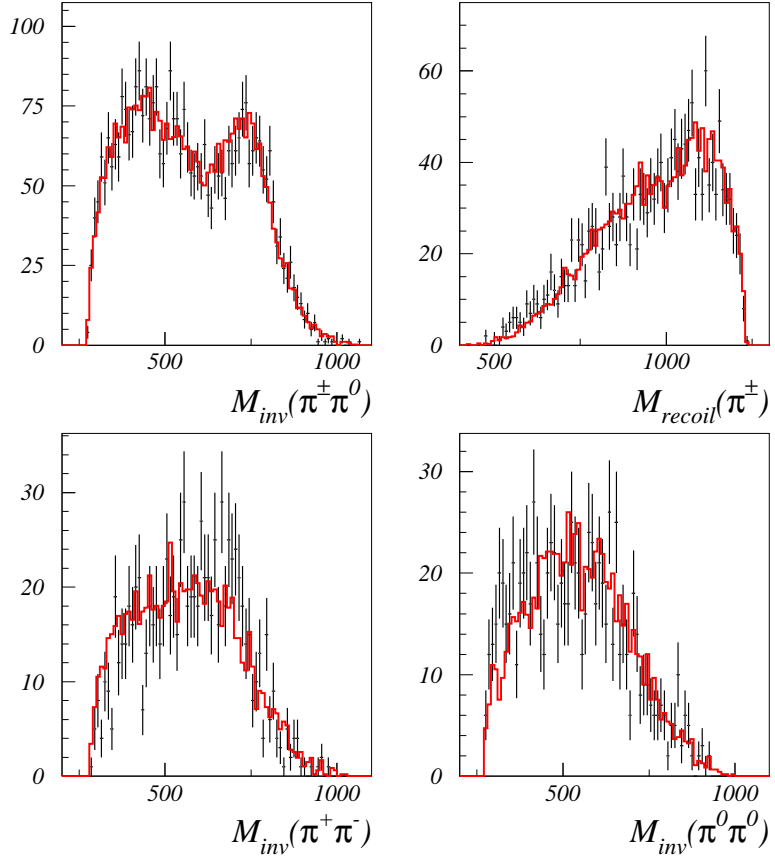


Figure 7: Distributions over  $M_{inv}(\pi^\pm\pi^0)$ ,  $M_{recoil}(\pi^\pm)$ ,  $M_{inv}(\pi^+\pi^-)$ ,  $M_{inv}(\pi^0\pi^0)$  for  $\pi^+\pi^-2\pi^0$  events from the class (II)

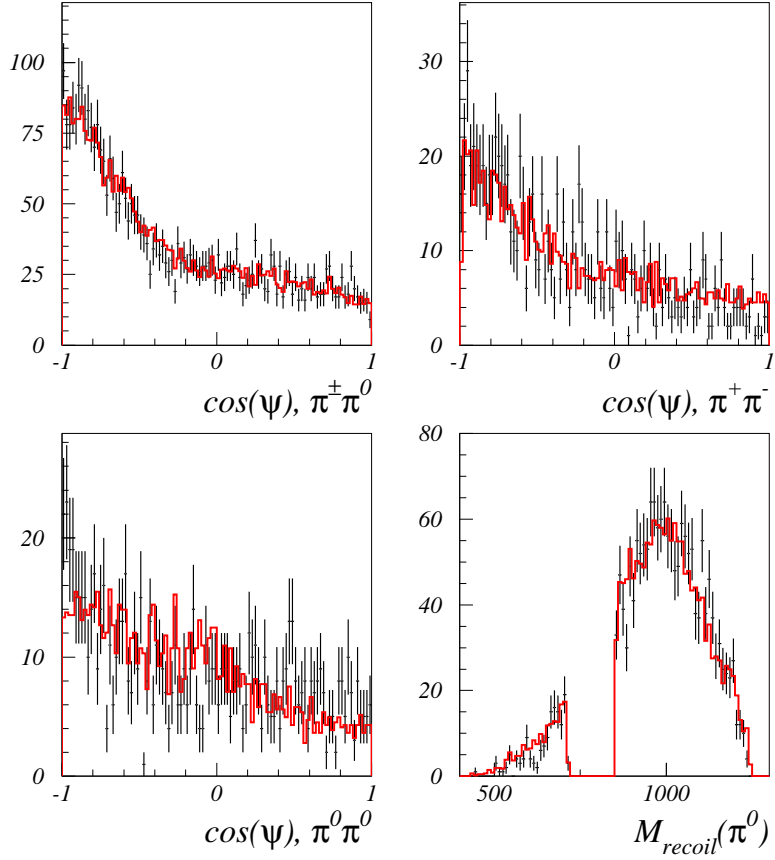


Figure 8: Distributions over  $\cos(\psi_{\pi^\pm\pi^0})$ ,  $\cos(\psi_{\pi^+\pi^-})$ ,  $\cos(\psi_{\pi^0\pi^0})$  and  $M_{recoil}(\pi^0)$  for  $\pi^+\pi^-2\pi^0$  events from the class (II)

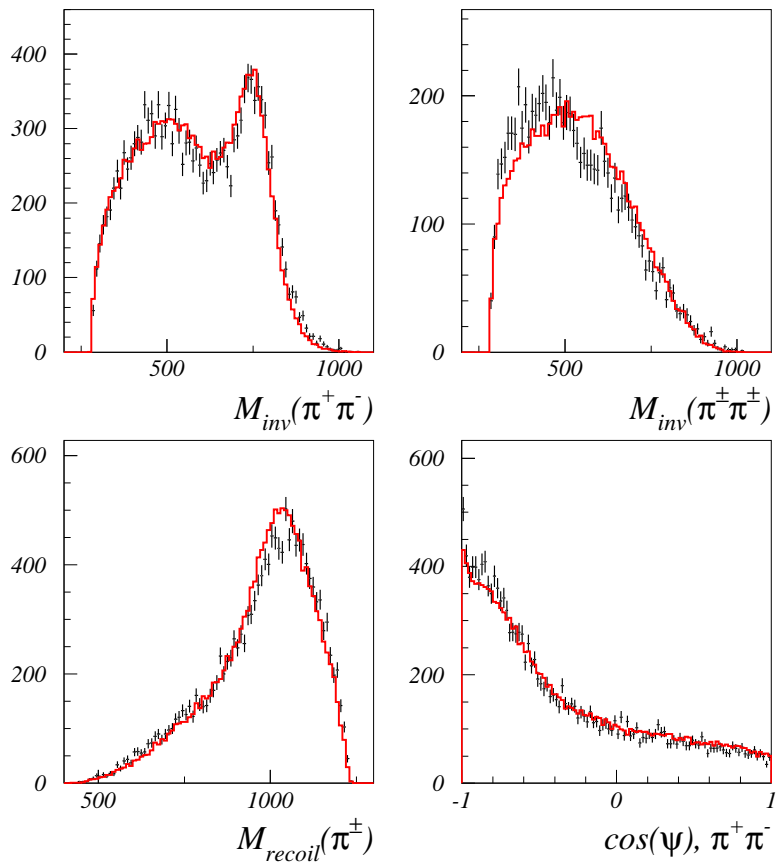


Figure 9: Distributions over  $M_{inv}(\pi^+\pi^-)$ ,  $M_{inv}(\pi^\pm\pi^\pm)$ ,  $M_{recoil}(\pi^\pm)$  and  $\cos(\psi_{\pi^+\pi^-})$  for  $4\pi^\pm$  events



### 3 Energy dependence of the cross sections

To obtain the  $a_1(1260)\pi$  contribution to the total cross section, we subtracted from the latter the contribution of the  $\omega\pi^0$  intermediate state. Strictly speaking, such a procedure loses its meaning when the interference between  $\omega\pi^0$  and  $a_1(1260)\pi$  is strong. In our case, however, the effects of the interference is numerically small ( $\sim 5\%$ ) because of the small width of the  $\omega$  meson.

In order to diminish the influence of background from soft photons, the additional cut was applied:  $\cos(\psi) < 0.7$  where  $\psi$  is the angle between the photon direction in the  $\pi^0$  rest frame and  $\pi^0$  momentum.

Cross sections were calculated from the formulae:

$$\begin{aligned}\sigma_{\omega\pi^0} &= \frac{N_\omega}{B(\omega \rightarrow 3\pi) \cdot (1 + \delta) \cdot L \cdot \epsilon}, \\ \sigma_{\pi^+\pi^-2\pi^0} &= \frac{N_{a_1}}{(1 + \delta) \cdot L \cdot \epsilon},\end{aligned}$$

where  $L$  is the luminosity,  $\epsilon$  is the detection efficiency from MC, and  $\delta$  is a radiative correction calculated according to [20].

$N_\omega$  and  $N_{a_1}$  are the numbers of events due to the corresponding reactions ( $e^+e^- \rightarrow \omega\pi^0$  and  $e^+e^- \rightarrow a_1\pi$  respectively) under the assumption that there is no interference. The values of  $N_\omega$  and  $N_{a_1}$  were determined from the equations:

$$\begin{aligned}N_1 &= N_\omega \cdot \alpha + N_{a_1} \cdot (1 - \beta), \\ N_2 &= N_\omega \cdot (1 - \alpha) + N_{a_1} \cdot \beta,\end{aligned}$$

where  $N_1$  and  $N_2$  are the numbers of events in the first and second classes respectively,  $\alpha$  is the probability for the  $\omega\pi^0$  event to enter the first class, and  $\beta$  is the probability for the  $a_1(1260)\pi$  event to enter the second class. The values of  $\alpha$  and  $\beta$  as a function of energy were taken from MC simulation.

Figure 10 shows the cross sections obtained for  $e^+e^- \rightarrow \omega\pi^0$  and  $e^+e^- \rightarrow \pi^+\pi^-2\pi^0$  with the  $\omega\pi^0$  contribution subtracted as explained above. Both cross sections rise with energy while the relative fraction of the  $a_1(1260)\pi$  increases.

Figure 11 shows the total cross section vs energy. Only statistical errors are shown. The systematic uncertainty for this channel consists of the contributions from the uncertainties in the event reconstruction, radiative corrections and luminosity determination. The overall systematic uncertainty was estimated to be  $\sim 15\%$ .

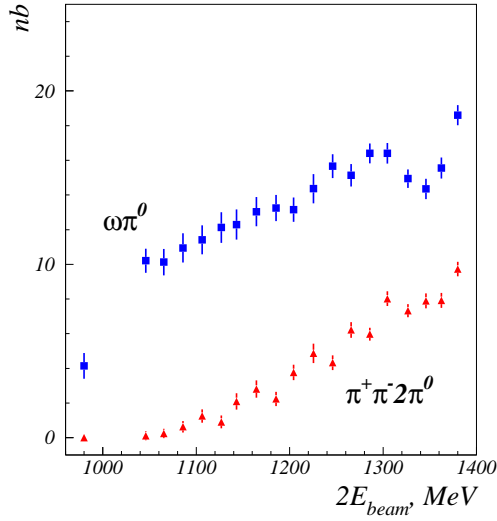


Figure 10: Energy dependence of  $\sigma(e^+e^- \rightarrow \omega\pi^0)$  and  $\sigma(e^+e^- \rightarrow \pi^+\pi^-2\pi^0)$  where the contribution of  $\omega\pi^0$  is subtracted

The cross section measured in our experiment is consistent with the previous measurement at OLYA [21] and within systematic errors does not contradict to the recent result from SND [22]. The value of the cross section from all three groups is significantly lower than that from ND [23, 24]. Also shown above 1.4 GeV are results from Orsay [15, 25] and Frascati [26] groups.

To determine the cross section  $e^+e^- \rightarrow 2\pi^+2\pi^-$  the following criteria were added:

- $\chi^2/ndf < 7$
- $\theta_{min} > 0.67$
- $|\sum_i E_i - 2 \cdot E_{beam}| < 0.2 \cdot E_{beam}$
- $|\sum_i \vec{p}_i| < 0.3 \cdot E_{beam}$

where  $E_i$ ,  $\vec{p}_i$  are pion energies and momenta before the kinematic reconstruction, and  $\theta_{min}$  is a minimal angle of pions with respect to the beam axis.

Figure 12 shows the total cross section vs energy. Only statistical errors are shown. The systematic uncertainty for this channel consists of the

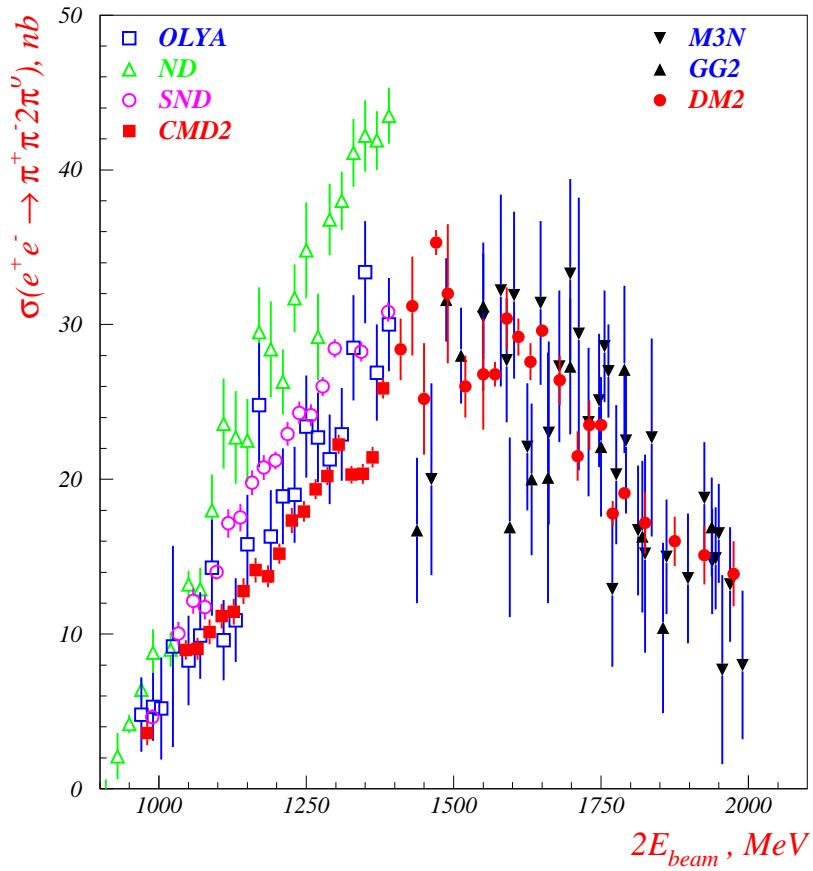


Figure 11: Energy dependence of the  $\pi^+\pi^-\pi^0$  cross section

contributions from the uncertainties in the event reconstruction, radiative corrections, selection criteria and luminosity determination. The overall systematic uncertainty was estimated to be  $\sim 15\%$ .

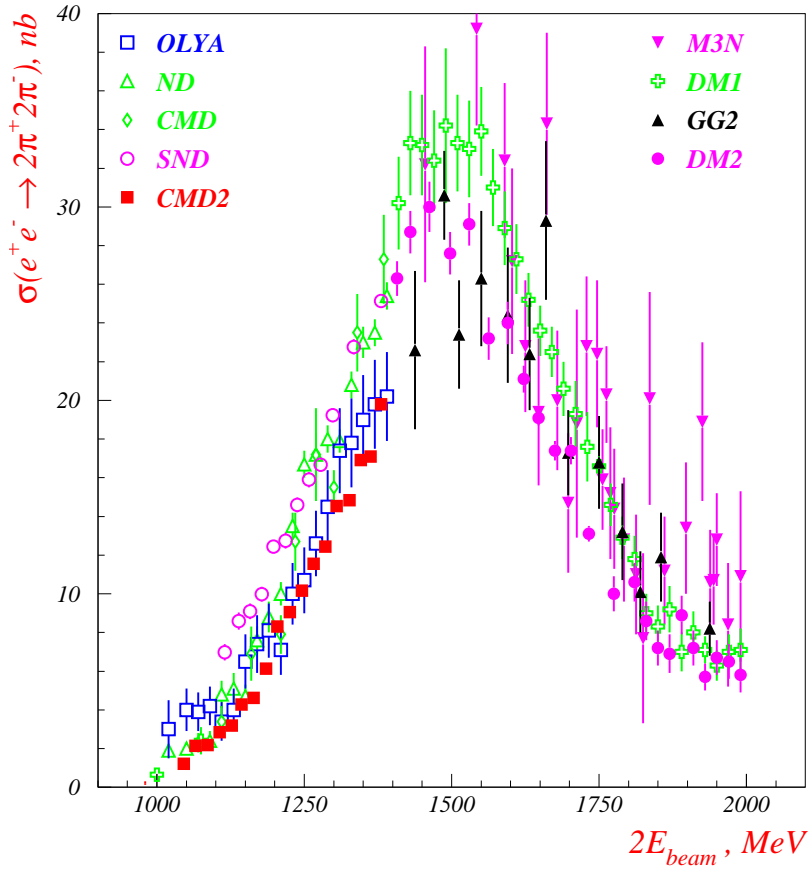


Figure 12: Energy dependence of the  $2\pi^+2\pi^-$  cross section

The obtained cross section is consistent with the previous measurements at OLYA [21], ND [23, 24] and CMD [10] and within systematic errors does not contradict to the recent result from SND [22]. Also shown above 1.4 GeV are results from Orsay [25, 8, 15] and Frascati [7, 27] groups.

Figure 13 presents the ratio of the cross sections  $\sigma(e^+e^- \rightarrow 2\pi^+2\pi^-)$  and

$\sigma(e^+e^- \rightarrow \pi^+\pi^-2\pi^0)$  where the contribution of  $\omega\pi^0$  is subtracted. The solid curve shows the theoretical prediction based on the  $a_1(1260)\pi$  dominance.

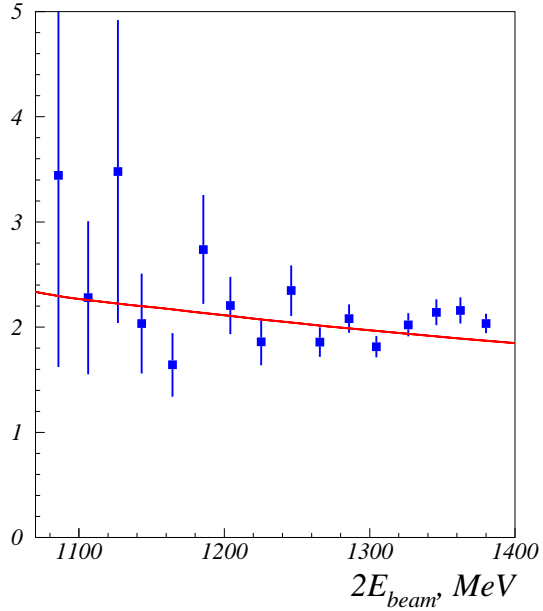


Figure 13: Energy dependence of the ratio  $\frac{\sigma(e^+e^- \rightarrow 2\pi^+2\pi^-)}{\sigma(e^+e^- \rightarrow \pi^+\pi^-2\pi^0)}$ . The contribution of  $\omega\pi^0$  is subtracted. The solid curve shows the theoretical prediction based on the  $a_1(1260)\pi$  dominance

In the energy range under consideration the experimentally measured ratio is about two. Calculations show that this ratio tends to four at very low energies close to the threshold of four pion production when the interference effects are maximal. The effects of interference decreases with energy since the produced resonances are moving at a high velocity. As a result, the ratio falls with energy and tends to unity.

The importance of the interference between the different diagrams corresponding to permutations of identical pions was first noted in [28]. The neglect of interference can lead to wrong conclusions about the contributions of different intermediate states to the total cross section.

## 4 Conclusion

The detailed analysis of the process  $e^+e^- \rightarrow \pi^+\pi^-2\pi^0$  unambiguously demonstrates that the dominant contribution to the cross section comes from  $\omega\pi^0$  and  $\rho^\pm\pi^\mp\pi^0$  intermediate states whereas the  $\rho^0\pi^0\pi^0$  state is not observed. Moreover, the  $\rho^\pm\pi^\mp\pi^0$  state is completely saturated by the  $a_1(1260)\pi$  mechanism. The latter also dominates in the cross section of the process  $e^+e^- \rightarrow 2\pi^+2\pi^-$ . This conclusion is based on the data sample corresponding to the integrated luminosity of  $5.8 \text{ pb}^{-1}$  collected with the CMD-2 detector in the energy range  $1.05 - 1.38 \text{ GeV}$ .

Comparison of the experimental data with the calculations shows that account of the interference of different amplitudes with various intermediate resonances but the identical final state drastically changes predictions for the differential distributions and total cross sections.

Through the hypothesis of CVC [2] experimentally tested to be valid within the 3-5% accuracy [3], we can relate the values of the four pion cross sections measured in  $e^+e^-$  to the hadronic spectra in corresponding four pion decays of the  $\tau$ -lepton. Moreover, our observation of the  $a_1(1260)\pi$  dominance should be also applied to  $\tau$ -lepton decays.

One should note that such a conclusion is in contradiction to that made by ARGUS collaboration [12]. However, their conclusion based on the distribution over the dipion mass is not compatible with the recent data from ALEPH [14]. The model used by ARGUS didn't take into account the interference of the amplitudes corresponding to various intermediate states whereas our observation unambiguously points to significance of the interference effects.

Our predictions for various two- and three-body invariant mass spectra will be addressed in more detail in the forthcoming paper which will compare them to the existing  $\tau$ -lepton data from ARGUS [12], CLEO [13] and ALEPH [14].

The detailed investigation of the energy behavior of exclusive channels of  $e^+e^-$  annihilation into hadrons is crucial for understanding the structure of the initial hadronic state created by the virtual photon ( $\rho(1450)$ ,  $\rho(1700)$  etc.). Our work considers this problem in the energy range below  $1.4 \text{ GeV}$ . At higher energy, such analysis can't be performed because  $e^+e^-$  annihilation data are not available now. One can hope to move forward by using data on semihadronic decays of the  $\tau$ -lepton.

Our statement about the  $a_1(1260)\pi$  dominance can be used for verification of theoretical models in which the problem of intermediate states has been discussed. In particular, recently there were numerous speculations about the possible existence of vector hybrids claiming that hybrids can be distinguished

from the normal  $q\bar{q}$  states by their decays, e.g. in the  $a_1(1260)\pi$  [29].

## Acknowledgements

The authors are grateful to the staff of VEPP-2M for excellent performance of the collider, to all engineers and technicians who participated in the design, commissioning and operation of CMD-2.

Special thanks are due to N.N. Achasov, M. Benayoun, V.L. Chernyak, V.F. Dmitriev, V.S. Fadin, V.B. Golubev, I.B. Khriplovich, L. Montanet, S.I. Serednyakov, A.I. Vainshtein for numerous discussions and constant interest.

# Appendix

## A Models of substructure in $e^+e^- \rightarrow 4\pi$

In this section we discuss the details of the model which has been used for description of the experimental data. Since the initial hadron state (referred to as  $\tilde{\rho}$ ) is created by a virtual photon ( $e^+e^- \rightarrow \gamma^* \rightarrow \tilde{\rho}$ ) and then decays into four pions, it has the  $\rho$ -meson quantum numbers ( $I^G J^{PC} = 1^+1^{--}$ ). We use the notation  $\tilde{e}_\mu$  for the polarization vector of this state.

We assume that the main contribution to the amplitude of the process in the energy range under study is given by the intermediate state resonances having the masses close to the threshold of  $\rho\pi$  production (1)-(7). In the case of broad resonances ( $a_1(1260), a_2(1320), \pi(1300)$  etc.), the form of their propagators  $1/D(q)$  is very important for analysing the data. We learned that it is necessary to take into account the dependence of the imaginary part of the propagators (width) on virtuality while the corresponding corrections to the real part which can be expressed through the imaginary part by dispersion relations are not so important.

We represent the function  $D(q)$  in the form

$$D(q) = q^2 - M^2 + iM\Gamma \frac{g(q^2)}{g(M^2)}, \quad (9)$$

where  $M$  and  $\Gamma$  are the mass and width of the corresponding particle, and the function  $g(s)$  describes the dependence of the width on the virtuality. If  $q^2 = M^2$  then  $D = iM\Gamma$ , in accordance with the usual definition of mass and width of the resonance. In the case of the  $\rho$ -meson we used the following representation for the function  $g_\rho(q)$ :

$$g_\rho(s) = s^{-1/2}(s - 4m^2)^{3/2}. \quad (10)$$

### A.1 The contribution of $a_1(1260)\pi$

The quantum numbers of the  $a_1(1260)$  resonance are  $I^G J^{PC} = 1^-1^{++}$ . Taking into account the quantum numbers of the pion, we can write the matrix elements corresponding to the processes  $\tilde{\rho}(P) \rightarrow a_1(q)\pi(p)$  and  $a_1(q) \rightarrow \rho(P')\pi(p)$  as

$$\begin{aligned} T(\tilde{\rho} \rightarrow a_1\pi) &= F_{\tilde{\rho}a_1\pi} \varepsilon^{3ab} (P_\mu \tilde{e}_\nu - P_\nu \tilde{e}_\mu) q_\mu A_\nu^{a*} \phi^{b*}, \\ T(a_1 \rightarrow \rho\pi) &= F_{a_1\rho\pi} \varepsilon^{abc} q_\mu A_\nu^a (P'_\mu \tilde{e}_\nu^{b*} - P'_\nu \tilde{e}_\mu^{b*}) \phi^{c*}, \end{aligned} \quad (11)$$



where  $a, b, c$  are isospin indices,  $A_\mu^a$  and  $e_\mu^a$  are the polarization vectors of  $a_1$ - and  $\rho$ -mesons,  $\phi^b$  is the pion wave function,  $F_{a_1\rho\pi}$  and  $F_{\tilde{\rho}a_1\pi}$  are form factors depending on the virtuality of initial and final particles. The explicit form of these form factors in the energy range considered is not very essential (it contributes to the theoretical uncertainty of the model). The matrix element of the transition  $T(\rho \rightarrow \pi\pi)$  reads

$$T(\rho \rightarrow \pi\pi) = F_{\rho\pi\pi} \varepsilon^{abc} e_\mu^a (p_\mu^{(b)} - p_\mu^{(c)}) \phi^{b*} \phi^{c*}, \quad (12)$$

where  $p_\mu^{(b)}$  and  $p_\mu^{(c)}$  are 4-momenta of the corresponding pions. Due to the helicity conservation only transverse space components (with respect to electron and positron momenta) of the 4-vector  $\tilde{e}_\mu$  are not zero. We denote them as  $\tilde{e}_\perp$ . For unpolarized electrons and positrons a square of matrix element for the process  $\tilde{\rho} \rightarrow 4\pi$  is of the form

$$|T|^2 = |\mathbf{J}_\perp|^2. \quad (13)$$

Using (11) and (12) we obtain the following expression for the contribution of the  $a_1(1260)$ -meson to the current  $\mathbf{J}$  in the process  $\tilde{\rho} \rightarrow \pi^+(p_1)\pi^+(p_2)\pi^-(p_3)\pi^-(p_4)$ :

$$\begin{aligned} \mathbf{J}_{a_1}^{++--} &= G [\mathbf{t}_{a_1}(p_1, p_2, p_3, p_4) + \mathbf{t}_{a_1}(p_1, p_4, p_3, p_2) + \mathbf{t}_{a_1}(p_2, p_1, p_3, p_4) \\ &\quad + \mathbf{t}_{a_1}(p_2, p_4, p_3, p_1) + \mathbf{t}_{a_1}(p_1, p_2, p_4, p_3) + \mathbf{t}_{a_1}(p_1, p_3, p_4, p_2) \\ &\quad + \mathbf{t}_{a_1}(p_2, p_1, p_4, p_3) + \mathbf{t}_{a_1}(p_2, p_3, p_4, p_1)], \end{aligned} \quad (14)$$

where

$$\begin{aligned} \mathbf{t}_{a_1}(p_1, p_2, p_3, p_4) &= \frac{F_{a_1}^2(P - p_4)}{D_{a_1}(P - p_4)D_\rho(p_1 + p_3)} \\ &\times \{ (E - \varepsilon_4)[\mathbf{p}_1(E\varepsilon_3 - p_4p_3) - \mathbf{p}_3(E\varepsilon_1 - p_4p_1)] \\ &\quad - \mathbf{p}_4[\varepsilon_1(p_4p_3) - \varepsilon_3(p_4p_1)] \}, \end{aligned} \quad (15)$$

$P$  is the initial 4-momentum ( $P^0 = E$ ,  $\mathbf{P} = 0$ ),  $p_i = (\varepsilon_i, \mathbf{p}_i)$ ,  $1/D_A(q)$  and  $1/D_\rho(q)$  are propagators of the  $a_1$ - and  $\rho$ -mesons,  $F_{a_1}(q)$  is the form factor,  $G$  is the function of the initial energy  $E$  proportional to the amplitude of  $\tilde{\rho}$  creation. Similarly to (14), we obtain for the contribution of  $a_1(1260)$  to the current  $\mathbf{J}$  in the process  $\tilde{\rho} \rightarrow \pi^+(p_1)\pi^-(p_4)\pi^0(p_2)\pi^0(p_3)$ :

$$\begin{aligned} \mathbf{J}_{a_1}^{+-00} &= G [\mathbf{t}_{a_1}(p_1, p_2, p_3, p_4) - \mathbf{t}_{a_1}(p_4, p_2, p_3, p_1) \\ &\quad + \mathbf{t}_{a_1}(p_1, p_3, p_2, p_4) - \mathbf{t}_{a_1}(p_4, p_3, p_2, p_1)]. \end{aligned} \quad (16)$$

The function  $g_{a_1}(s)$  in the propagator of  $a_1$  reads:

$$g_{a_1}(s) = F_{a_1}^2(Q) \int \left| \frac{\varepsilon_2 \mathbf{p}_1 - \varepsilon_1 \mathbf{p}_2}{D_\rho(p_1 + p_2)} + \frac{\varepsilon_2 \mathbf{p}_3 - \varepsilon_3 \mathbf{p}_2}{D_\rho(p_2 + p_3)} \right|^2 \times \frac{d\mathbf{p}_1 d\mathbf{p}_2 d\mathbf{p}_3 \delta^{(4)}(p_1 + p_2 + p_3 - Q)}{2\varepsilon_1 2\varepsilon_2 2\varepsilon_3 (2\pi)^5}, \quad (17)$$

where  $Q^0 = \sqrt{s}$  and  $\mathbf{Q} = 0$ . As a form factor, we used the function  $F(q) = (1 + m_{a_1}^2/\Lambda^2)/(1 + q^2/\Lambda^2)$  with  $\Lambda \sim 1$  GeV.

## A.2 The contribution of $\omega\pi$

The amplitude of the process  $\tilde{\rho}(\mathcal{P}) \rightarrow \omega(q)\pi(p)$  has the form:

$$T(\tilde{\rho} \rightarrow \omega\pi) = F_{\tilde{\rho}\omega\pi} \varepsilon_{\mu\nu\alpha\beta} \mathcal{P}_\mu q_\nu \tilde{e}_\alpha^a e_\beta^a, \quad (18)$$

where  $e_\beta^a$  is the polarization vector of the  $\omega$ -meson. The matrix element of the transition  $\omega \rightarrow \rho\pi$  can be written in the similar form. The  $\omega$ -meson contributes only to a channel  $\tilde{\rho} \rightarrow \pi^+(p_1)\pi^-(p_4)\pi^0(p_2)\pi^0(p_3)$ . The corresponding current is equal to

$$\mathbf{J}_\omega^{+-00} = G_\omega [\mathbf{t}_\omega(p_2, p_4, p_1, p_3) - \mathbf{t}_\omega(p_2, p_1, p_4, p_3) - \mathbf{t}_\omega(p_2, p_3, p_1, p_4)] + (p_2 \leftrightarrow p_3), \quad (19)$$

where

$$\mathbf{t}_\omega(p_1, p_2, p_3, p_4) = \frac{F_\omega^2(P - p_1)}{D_\omega(P - p_1)D_\rho(p_3 + p_4)} \times \{(\varepsilon_4 \mathbf{p}_3 - \varepsilon_3 \mathbf{p}_4)(\mathbf{p}_1 \mathbf{p}_2) - \mathbf{p}_2(\varepsilon_4 \mathbf{p}_1 \mathbf{p}_3 - \varepsilon_3 \mathbf{p}_1 \mathbf{p}_4) - \varepsilon_2[\mathbf{p}_3(\mathbf{p}_1 \mathbf{p}_4) - \mathbf{p}_4(\mathbf{p}_1 \mathbf{p}_3)]\}, \quad (20)$$

$\varepsilon_i$  is the energy of the corresponding pion,  $F_\omega(q)$  is the form factor. Since the width of the  $\omega$  is small, we set  $g_\omega(s) = 1$  in the propagator  $D_\omega(q)$ .

## A.3 The contribution of $h_1(1170)\pi$

The quantum numbers of the  $h_1(1170)$  resonance are  $I^G J^{PC} = 0^- 1^{+-}$ . Similarly to the  $\omega$ -meson it gives the contribution to the mixed channel only. The matrix elements for the transitions  $\tilde{\rho}(P) \rightarrow h_1(q)\pi^0(p)$  and  $h_1(q) \rightarrow \rho(P)\pi(p)$  have the form

$$\begin{aligned} T(\tilde{\rho} \rightarrow h_1\pi^0) &= F_{\tilde{\rho}h_1\pi} (P_\mu \tilde{e}_\nu - P_\nu \tilde{e}_\mu) q_\mu H_\nu^* \phi^{3*}, \\ T(h_1 \rightarrow \rho\pi) &= F_{h_1\rho\pi} q_\mu H_\nu (P_\mu e_\nu^{a*} - P_\nu e_\mu^{a*}) \phi^{a*}, \end{aligned} \quad (21)$$

where  $H_\mu$  is the polarization vector of  $h_1$ . Using (21) and (12) we obtain the following representation for the  $h_1$ -meson contribution to the current  $\mathbf{J}$  in the decay  $\tilde{\rho} \rightarrow \pi^+(p_1)\pi^-(p_4)\pi^0(p_2)\pi^0(p_3)$  :

$$\mathbf{J}_{h_1}^{+-00} = G_{h_1} [\mathbf{t}_{h_1}(p_1, p_4, p_3, p_2) - \mathbf{t}_{h_1}(p_4, p_1, p_3, p_2) - \mathbf{t}_{h_1}(p_1, p_3, p_4, p_2)] + (p_2 \leftrightarrow p_3), \quad (22)$$

the current  $\mathbf{t}_{h_1}$  is given by (15) with the change of indices  $a_1 \rightarrow h_1$ , and the function  $g_{h_1}(s)$  in the propagator of  $h_1$  is:

$$g_{h_1}(s) = F_{h_1}^2(Q) \int \left| \frac{\varepsilon_2 \mathbf{P}_1 - \varepsilon_1 \mathbf{P}_2}{D_\rho(p_1 + p_2)} - \frac{\varepsilon_2 \mathbf{P}_3 - \varepsilon_3 \mathbf{P}_2}{D_\rho(p_2 + p_3)} - \frac{\varepsilon_3 \mathbf{P}_1 - \varepsilon_1 \mathbf{P}_3}{D_\rho(p_1 + p_3)} \right|^2 \times \frac{d\mathbf{p}_1 d\mathbf{p}_2 d\mathbf{p}_3 \delta^{(4)}(p_1 + p_2 + p_3 - Q)}{2\varepsilon_1 2\varepsilon_2 2\varepsilon_3 (2\pi)^5}. \quad (23)$$

#### A.4 The contribution of $\rho^+\rho^-$

One more contribution to the mixed channel amplitude comes from the process  $\tilde{\rho} \rightarrow \rho^+\rho^- \rightarrow 4\pi$ . The matrix element corresponding to the transition  $\tilde{\rho}(P) \rightarrow \rho^+(p)\rho^-(q)$  reads

$$T(\tilde{\rho} \rightarrow \rho^+\rho^-) = F_{\tilde{\rho}\rho^+\rho^-} (P_\mu \tilde{e}_\nu - P_\nu \tilde{e}_\mu) \times [(p_\mu e_\alpha^{+*} - p_\alpha e_\mu^{+*})(q_\nu e_\alpha^{-*} - q_\alpha e_\nu^{-*}) - (\mu \leftrightarrow \nu)] \quad (24)$$

where  $e_\mu^+$  and  $e_\mu^-$  are the polarization vectors of  $\rho^+$  and  $\rho^-$  respectively. Using (24), we obtain the contribution of  $\rho^+\rho^-$  to the current  $\mathbf{J}$  in the decay  $\tilde{\rho} \rightarrow \pi^+(p_1)\pi^-(p_4)\pi^0(p_2)\pi^0(p_3)$  :

$$\mathbf{J}_{\rho\rho}^{+-00} = \frac{G_{\rho\rho} F_\rho^2(p_1 + p_2) F_\rho^2(p_3 + p_4)}{D_\rho(p_1 + p_2) D_\rho(p_3 + p_4)} \times [\mathbf{p}_1(\varepsilon_3 \mathbf{p}_2 \mathbf{p}_4 - \varepsilon_4 \mathbf{p}_2 \mathbf{p}_3) - \mathbf{p}_2(\varepsilon_3 \mathbf{p}_1 \mathbf{p}_4 - \varepsilon_4 \mathbf{p}_1 \mathbf{p}_3) - \mathbf{p}_3(\varepsilon_1 \mathbf{p}_2 \mathbf{p}_4 - \varepsilon_2 \mathbf{p}_1 \mathbf{p}_4) + \mathbf{p}_4(\varepsilon_1 \mathbf{p}_2 \mathbf{p}_3 - \varepsilon_2 \mathbf{p}_1 \mathbf{p}_3)] + (2 \leftrightarrow 3). \quad (25)$$

#### A.5 The contribution of $\pi(1300)\pi$

The matrix elements for the transitions  $\tilde{\rho}(P) \rightarrow \pi'(q)\pi(p)$  and  $\pi'(q) \rightarrow \rho(P)\pi(p)$  are of the form (for brevity  $\pi' \equiv \pi(1300)$ ):

$$\begin{aligned} T(\tilde{\rho} \rightarrow \pi'\pi) &= F_{\tilde{\rho}\pi'\pi} \varepsilon^{3ab} (P_\mu \tilde{e}_\nu - P_\nu \tilde{e}_\mu) q_\mu p_\nu \phi'^{a*} \phi^{b*}, \\ T(\pi' \rightarrow \rho\pi) &= F_{\pi'\rho\pi} \varepsilon^{abc} q_\mu p_\nu (P_\mu e_\nu^{b*} - P_\nu e_\mu^{b*}) \phi'^{a} \phi^{c*}. \end{aligned} \quad (26)$$

Then we get for the contribution of  $\pi(1300)$  to the current  $\mathbf{J}$  in the decay  $\tilde{\rho} \rightarrow \pi^+(p_1)\pi^+(p_2)\pi^-(p_3)\pi^-(p_4)$  :

$$\begin{aligned} \mathbf{J}_{\pi'}^{++++} &= G_{\pi'} [\mathbf{t}_{\pi'}(p_1, p_2, p_3, p_4) + \mathbf{t}_{\pi'}(p_2, p_1, p_3, p_4) + \mathbf{t}_{\pi'}(p_1, p_2, p_4, p_3) \\ &\quad + \mathbf{t}_{\pi'}(p_2, p_1, p_4, p_3) + \mathbf{t}_{\pi'}(p_3, p_2, p_1, p_4) + \mathbf{t}_{\pi'}(p_4, p_2, p_1, p_3) \\ &\quad + \mathbf{t}_{\pi'}(p_3, p_1, p_2, p_4) + \mathbf{t}_{\pi'}(p_4, p_1, p_2, p_3)] . \end{aligned} \quad (27)$$

In the mixed channel  $\tilde{\rho} \rightarrow \pi^+(p_1)\pi^-(p_4)\pi^0(p_2)\pi^0(p_3)$  the corresponding current reads:

$$\begin{aligned} \mathbf{J}_{\pi'}^{+-00} &= G_{\pi'} [\mathbf{t}_{\pi'}(p_1, p_2, p_3, p_4) + \mathbf{t}_{\pi'}(p_1, p_3, p_2, p_4) \\ &\quad + \mathbf{t}_{\pi'}(p_4, p_1, p_3, p_2) + \mathbf{t}_{\pi'}(p_4, p_1, p_2, p_3)] . \end{aligned} \quad (28)$$

It (27) and (28) we use the notation

$$\mathbf{t}_{\pi'}(p_1, p_2, p_3, p_4) = \frac{F_{\pi'}^2(P - p_1)}{D_{\pi'}(P - p_1)D_{\rho}(p_2 + p_4)}(p_2p_3 - p_4p_3)(p_2 + p_4)^2 \mathbf{p}_1 . \quad (29)$$

For the function  $g_{\pi'}(s)$  in the  $\pi'$  propagator, one has:

$$\begin{aligned} g_{\pi'}(s) &= F_{\pi'}^2(Q) \int \left| \frac{\varepsilon_1 \mathbf{p}_2 \mathbf{p}_3 - \varepsilon_2 \mathbf{p}_1 \mathbf{p}_3}{D_{\rho}(p_1 + p_2)} + \frac{\varepsilon_3 \mathbf{p}_1 \mathbf{p}_2 - \varepsilon_2 \mathbf{p}_1 \mathbf{p}_3}{D_{\rho}(p_2 + p_3)} \right|^2 \\ &\quad \times \frac{d\mathbf{p}_1 d\mathbf{p}_2 d\mathbf{p}_3 \delta^{(4)}(p_1 + p_2 + p_3 - Q)}{2\varepsilon_1 2\varepsilon_2 2\varepsilon_3 (2\pi)^5} . \end{aligned} \quad (30)$$

## A.6 The contribution of $\sigma\rho$

The quantum numbers of the  $\sigma$  resonance are  $I^G J^{PC} = 0^+ 0^{++}$ . The matrix element of the transition  $\tilde{\rho}(P) \rightarrow \sigma(q)\rho^0(p)$  is of the form:

$$T(\tilde{\rho} \rightarrow \sigma\rho^0) = F_{\tilde{\rho}\sigma\rho}(P_{\mu}\tilde{e}_{\nu} - P_{\nu}\tilde{e}_{\mu})q_{\mu}e_{\nu}^*\phi_{\sigma}^* . \quad (31)$$

The corresponding contribution to the current  $\mathbf{J}$  in the decay  $\tilde{\rho} \rightarrow \pi^+(p_1)\pi^+(p_2)\pi^-(p_3)\pi^-(p_4)$  reads:

$$\begin{aligned} \mathbf{J}_{\sigma}^{++++} &= G_{\sigma} [\mathbf{t}_{\sigma}(p_1, p_2, p_3, p_4) + \mathbf{t}_{\sigma}(p_2, p_1, p_3, p_4) \\ &\quad + \mathbf{t}_{\sigma}(p_1, p_2, p_4, p_3) + \mathbf{t}_{\sigma}(p_2, p_1, p_4, p_3)] . \end{aligned} \quad (32)$$

In the mixed channel  $\tilde{\rho} \rightarrow \pi^+(p_1)\pi^-(p_4)\pi^0(p_2)\pi^0(p_3)$  the current has the form

$$\mathbf{J}_{\sigma}^{+-00} = G_{\sigma} \mathbf{t}_{\sigma}(p_1, p_2, p_3, p_4) , \quad (33)$$

where

$$\mathbf{t}_\sigma(p_1, p_2, p_3, p_4) = \frac{F_\sigma^2(p_2 + p_3)}{D_\sigma(p_2 + p_3)D_\rho(p_1 + p_4)}(\varepsilon_4 \mathbf{P}_1 - \varepsilon_1 \mathbf{P}_4). \quad (34)$$

The function  $g_\sigma(s)$  in the propagator of  $\sigma$  is equal to

$$g_\sigma(s) = (1 - 4m^2/s)^{1/2}. \quad (35)$$

## A.7 The contribution of $a_2(1320)\pi$

The quantum numbers of the  $a_2(1320)$  resonance are  $I^G J^{PC} = 1^- 2^{++}$ . The matrix elements for the transitions  $\tilde{\rho}(P) \rightarrow a_2(q)\pi(p)$  and  $a_2(q) \rightarrow \rho(P')\pi(p)$  can be written in the form

$$\begin{aligned} T(\tilde{\rho} \rightarrow a_2\pi) &= F_{\tilde{\rho}a_2\pi} \varepsilon^{3ab} \varepsilon_{\mu,\nu\rho\lambda} P_\mu \tilde{e}_\nu p_\rho A_{\lambda\gamma}^{a*} p_\gamma q_\mu \phi^{b*}, \\ T(a_2 \rightarrow \rho\pi) &= F_{a_2\rho\pi} \varepsilon^{abc} \varepsilon_{\mu,\nu\rho\lambda} P'_\mu e_\nu^{a*} p_\rho A_{\lambda\gamma}^b p_\gamma \phi^{c*} \end{aligned} \quad (36)$$

where  $A_{\mu\nu}^a$  is the polarization tensor of  $a_2$ . The contributions of the  $a_2$ -meson to the current  $\mathbf{J}$  in the processes  $\tilde{\rho} \rightarrow \pi^+(p_1)\pi^+(p_2)\pi^-(p_3)\pi^-(p_4)$  and  $\tilde{\rho} \rightarrow \pi^+(p_1)\pi^-(p_4)\pi^0(p_2)\pi^0(p_3)$  are given by the formulae (14) and (16) with the substitution  $\mathbf{t}_{a_1} \rightarrow \mathbf{t}_{a_2}$ , where

$$\begin{aligned} \mathbf{t}_{a_2}(p_1, p_2, p_3, p_4) &= \frac{F_{a_2}^2(P - p_4)}{D_A(P - p_4)D_\rho(p_1 + p_3)} \\ &\times \{E(\mathbf{p}_4 \times \mathbf{p}_2)[\mathbf{p}_1 \times \mathbf{p}_3, \mathbf{p}_2] + [p_2 p_4 - (p_2 q)(p_4 q)/m_{a_2}^2] \\ &\times [\mathbf{p}_1(\varepsilon_3 \mathbf{p}_2 \mathbf{p}_4 - \varepsilon_2 \mathbf{p}_4 \mathbf{p}_3) - \mathbf{p}_3(\varepsilon_1 \mathbf{p}_4 \mathbf{p}_2) - \varepsilon_2 \mathbf{p}_4 \mathbf{p}_1 \\ &+ \mathbf{p}_2(\varepsilon_1 \mathbf{p}_3 \mathbf{p}_4 - \varepsilon_3 \mathbf{p}_1 \mathbf{p}_4)]\}. \end{aligned} \quad (37)$$

Here  $q = P - p_4$ , and  $P$  is the initial 4-momentum.

For the function  $g_{a_2}(s)$  in the propagator of  $a_2$ , we obtain:

$$g_{a_2}(s) = F_{a_2}^2(Q) \int \mathcal{F}_{ij} \mathcal{F}_{ij}^* \frac{d\mathbf{p}_1 d\mathbf{p}_2 d\mathbf{p}_3 \delta^{(4)}(p_1 + p_2 + p_3 - Q)}{2\varepsilon_1 2\varepsilon_2 2\varepsilon_3 (2\pi)^5}, \quad (38)$$

where

$$\mathcal{F}_{ij}(s) = \frac{(\mathbf{p}_2 \times \mathbf{p}_3)^i \mathbf{p}_1^j}{D_\rho(p_2 + p_3)} + \frac{(\mathbf{p}_1 \times \mathbf{p}_3)^i \mathbf{p}_2^j}{D_\rho(p_1 + p_3)} + (i \leftrightarrow j) \quad (39)$$

## References

- [1] S.Eidelman and F.Jegerlehner, Z. Phys. **C67** (1995) 585.
- [2] Y.S.Tsai, Phys. Rev. **D4** (1971) 2821.  
H.B.Thacker and J.J.Sakurai, Phys. Lett. **B36** (1971) 103.
- [3] S.I.Eidelman and V.N.Ivanchenko, Phys. Lett. **B257** (1991) 437.
- [4] M.A.Shifman, A.I.Vainshtein, V.I.Zacharov, Nucl. Phys. **B147** (1979) 385.
- [5] B.Bartoli *et al.*, Nuovo Cim. **70A** (1970) 615.
- [6] L.M.Kurdadze *et al.*, Phys. Lett. **42B** (1972) 515.
- [7] B.Esposito *et al.*, Lett. Nuovo Cim. **28** (1980) 195.
- [8] A.Cordier *et al.*, Phys. Lett. **109B** (1982) 129.
- [9] L.M.Kurdadze *et al.*, JETP Lett. **47** (1988) 512.
- [10] L.M.Barkov *et al.*, Sov. J.Nucl. Phys. **47** (1988) 248.
- [11] S.I.Dolinsky *et al.*, Phys. Lett. **B174** (1986) 453.
- [12] H.Albrecht *et al.*, Phys. Lett. **B185** (1987) 223. H.Albrecht *et al.*, Phys. Lett. **B260** (1991) 259.
- [13] R.Balest *et al.*, Phys. Rev. Lett. **75** (1995) 3809.
- [14] D.Busculic *et al.*, Zeit. f. Phys. **C74** (1997) 263.
- [15] D.Bisello *et al.*, Preprint LAL-91-64, Orsay, 1991.
- [16] G.A.Aksenov *et al.*, Preprint BudkerINP 85-118, Novosibirsk, 1985.  
E.V. Anashkin *et al.*, ICFA Instrumentation Bulletin **5** (1988)18.
- [17] G.I.Kopylov, Basic kinematics of resonances, Science Publ. House, Moscow, 1970 (in Russian).
- [18] F.James, MINUIT - Function Minimization and Error Analysis, CERN Program Library, 1994.
- [19] E.V.Anashkin *et al.*, Preprint BudkerINP 99-1, Novosibirsk, 1999.
- [20] E.A.Kuraev and V.S.Fadin, Sov. J. Nucl. Phys. **41** (1985) 466.

- [21] L.M.Kurdadze *et al.*, JETP Lett. **43** (1986) 643.
- [22] M.N.Achasov *et al.*, Preprint BudkerINP 98-65, Novosibirsk, 1998.
- [23] V.M.Aulchenko *et al.*, Preprint INP 86-106, Novosibirsk, 1986.
- [24] S.I. Dolinsky *et al.*, Phys. Rep. **202** (1991) 99.
- [25] G.Cosme *et al.*, Nucl. Phys. **B152** (1979) 215.
- [26] C.Bacci *et al.*, Nucl. Phys. **B184** (1981) 31.
- [27] C.Bacci *et al.*, Phys. Lett. **95B** (1980) 139.
- [28] S.I.Eidelman, JETP Lett. **26** (1977) 417.
- [29] F.Close, P.Page, Nucl. Phys. **B443** (1995) 233.  
T.Barnes *et al.*, Phys. Rev. **D55** (1997) 4157.